

Cooperative and Low-Power Wireless Sensor Network for Efficient Body-Centric Communications in Healthcare Applications

Raffaele Di Bari, Akram Alomainy, and Yang Hao

Antennas and Electromagnetics Research Group
School of Electronic Engineering and Computer Science
Queen Mary, University of London
Mile End Road, London E1 4NS, UK
akram.alomainy@eecs.qmul.ac.uk

Abstract. Body Sensor Networks are an interesting emerging application to improve healthcare and the quality of life monitoring. In this paper, we compare the performances of multi-hop cooperative and single-hop networks with real-world sensor networks based on Zigbee technology. The network reliability, the data flow rate, the packet delivery ratio and the energy consumption are included as performances criteria. It is shown experimentally that the cooperative approach can provide a network more robust to link losses at the expenses of a lower bit rate and higher energy consumption. Specifically, for a packet delivery ratio >0.9 , the cooperative scheme can provide the network with a link gain up to 14 dB traded off with an energy demand up to 30.7% higher and a data flow rate about 20% lower than a single-hop system. This work is a first exercise step in assessing reliability and life time trade-off with real-world platforms for body area sensor networks. Follow-up studies will address wireless ECG emulators with higher number of sensors (e.g. up to 10 for a typical 12-leads ECG system) employing ultra-low power chipsets in different specific health monitoring environments.

Keywords: Body-centric wireless communication, co-operative networks, energy efficiency, healthcare monitoring.

1 Introduction

Research on sensor network has been carried out using small, low-power digital radios based on an IEEE 802.15 standard [1], a high-level communication protocols suitable for WBANs [2-3]. The most straightforward approach to deploy a WBAN is considering single-hop (SH) communications between sensors and the sink. However, the body impact on the signal can result in severe path losses, even larger than 50dB [4]. Due to these high losses, direct communication between the sensors and the sink will not always be convenient (or even possible), especially when extended sensor lifetime is targeted deploying ultra-low range transceivers [5].

In a relay MH network, each sensor is dedicated to transmit or relay information packets, while in cooperative MH network each sensor can perform both operations. An example of MH WBAN benefits is introduced in [10], where spatial diversity gain is analyzed for a two-relay assisted transmission link, while a tree cross-layer protocols such as CICADA [11] and WASP scheme [12] aimed to achieve WBANs reliability and low delay, although no considerable attention is focused on balancing the power consumption between the interconnected sensors [13]. Several researchers also attempted to design energy-aware MH protocols, considering also different metrics such as delay and reliability as Quality of Service requirements [14-17]. Although these studies show that MH communications are suitable to overcome link blockage in sensor WBANs, the MH energy efficiency compared to the SH schemes is still an open issue and depends on several system parameters, including chipset implementation, sensors distance, and network topologies. A recent network design proposed in [18], shows a significant increase in battery life for relay MH scenarios considering only the transmit power.

The main objective of this paper is to compare experimentally the performances of MH cooperative and SH schemes for a WBAN. The power margins, the data flow rate, the sensor packet delivery ratio (PDR) and the average energy consumption are selected as a main performance criterion. The sensors generate and transmit data at regular intervals with a data flow rate suitable for ECG constant monitoring system.

2 Practical Considerations of the Body Sensor Network

A prototype synchronous sensor network at 2.4 GHz is set-up, where each sensor consists of a Sentilla Perk mote [22], standard compliant with the IEEE 802.15.4/Zigbee protocol. A total number of 4 sensors (with index $i = 1, 2, 3$ and 4) were placed on human volunteer (each attached on head, left leg, left wrist, and back) in sitting postural as shown in Fig. 1, while a sensor acting as sink is placed in the waist area. This is a representative scenario for patients who are resting for a major part of the day. The sensor 4 is placed on the volunteer's back diametrically opposite sensor 3. The sensors are placed such that batteries are closest to skin, with the antennas being further away. With respect to the sink, two sensors are in quasi-LOS (e.g. 1 and 2) while two others are in NLOS (e.g. 3 and 4). Experiments were run in office indoor scenario.

The sink collects raw data, and sends statistics to an off-body server using a wireless link. The network operations can ideally be cyclically repeated and they can be divided in 3 main phases: (1) setting-up of the routing tree topology, (2) time-slot transmission synchronization, and (3) data transmission. A time-synchronous architecture approach was selected as best suited to maximize the data delivery ratio. The first two phases can be ranked as start-up phases, the latter as steady-state phase. The sensors send routing messages in phase 1, dummy messages in phase 2 for synchronization purposes, and actual data messages during phase 3. The network performs cycles of the 3 phases with periodicity T_N to adapt its topology to the body movements and postural and environment changes.

2.1 Topology Update (Phase A)

The Minimum Cost Forwarding (MCF) network routing protocol [23] has been implemented on the top of the standard connection functionality provided by the Sentilla motes kit. The routing algorithm adopted seeks to achieve minimum cost from each sensor toward the sink, where costs are proportional to the RSSI. In SH case, each sensor transmits by default to the sink so no routing data is required, while in MH protocol case, each sensor retains the next hop target sensor address to build the tree topology. From previous published works [24, 28], the RSSI seems to provide a good estimation of packet loss rates; e.g. RSSI of -90 dBm or larger always corresponds to a PDR of 95% or more. The RSSI comes from the CC2420 built-in register, whose values are estimated in accordance to [1]. The RSSI register value $RSSI_{VAL}$ can be referred to the power P_{RF} at the RF pins by using the following equations:

$$P_{RF} = RSSI_{VAL} + RSSI_{OFFSET} \quad (1)$$

where the $RSSI_{OFFSET}$ is approximately -45 (e.g. if reading a value of -20 from the $RSSI_{VAL}$ register, the P_{RF} is approximately -65 dBm). The $RSSI_{VAL}$ can directly be related to the path loss L_P and to the transmit power P_{TX} according

$$RSSI_{VAL} = P_{TX} - L_P - RSSI_{OFFSET} \quad (2)$$

As transmit and receive antenna gain cannot be explicitly estimated because of the relative orientation and body impact, they are considered as embedded in the L_P term. The PRF values are not numerically suitable as link costs for the routing algorithm. In fact, the sum of any MH links combination will not be lower than the SH links, even for MH power-wise convenient routes.

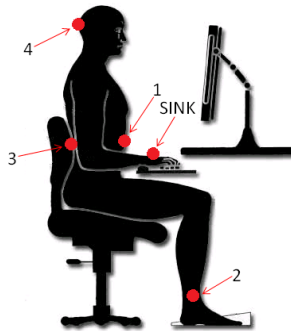


Fig. 1. Displacement map of 4 sensors and a sink network on volunteer body

2.2 Synchronisation (Phase B)

The transmit time slots are synchronised in Phase 2 using beacons with a unique sensor address periodically sent by the sink. In this phase, each sensor is constantly in

receiving mode, listening for sink beacons and other sensor messages. If a beacon is received, the sensor set up a wake-up timer and send a packet to the next hop target sensor (or to the sink in case of SH scheme). If a sensor receives a message, it simply relays to the next hop. Thus, the sink and the sensors involved in relaying can synchronize their wake-up timers for receiving the messages from neighbourhood sensors. As the sink knows the total number of sensors (but not the network topology nor the latency *a priori*), it does not send a new beacon until a packet is received from the target sensor. As the message delay depends of number of hops, R is expected to lower in MH scheme. After phase 2, the sink and the sensor have set a wake-up time, and no beacons are required anymore.

2.3 Transmission (Phase C)

At the end of phase 2, the communication between sensors is time-slotted according the wake up times to avoid idle listening and save energy. Each sensor regularly transmits data packets of 75 bytes of payload. In case of MH protocol, a sensor relays messages from neighbourhood sensors immediately after reception, with no data buffering. The sensor operation type (e.g. transmit or transmit and relay) depends on the network topology and it can dynamically change every cycle T_N . Considering a sensor in transmit operation type as shown in Fig. 2, the communication tasks are divided into 3 time slots: in T_P , the sensor generate data to transmit, in T_{TX} the sensor transmit the data packets, while in T_S the sensor is in sleeping mode. T_{TX} is fixed and empirically estimated to be ~ 108 ms. This value includes value data serialization, a method of transforming Java objects into a byte stream (binary form), so they can be sent and received over the radio. Thus, the actual time required to transmit data itself is < 100 ms. The sensor sleeping time is T_S and it varies according the synchronisations, while the active time is defined as $T_A = T_{TX} + T_P$, where T_P is ~ 72 ms.

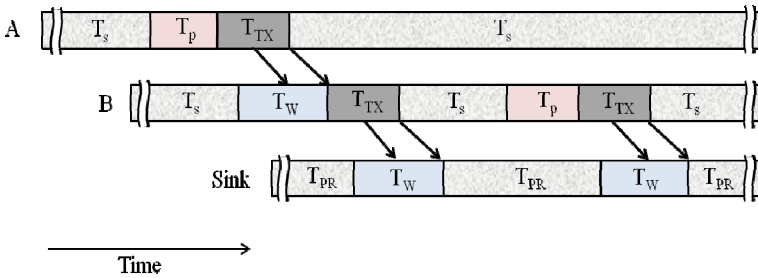


Fig. 2. Packet data communication tasks for a (A) transmit sensor, (B) relay sensor and Sink sensors operation modes (blocks are not in scale)

3 Experimental Investigations and Analyses

This section presents the results of the real-world tests. Considering a static posture of the patient, we assume a constant time average for RSSI is assumed per each link.

Each body link has been preliminary characterized in terms of measured average RSSI; data are stored in the devices memory and associated to each link before the experiments. As the links costs are now fixed, a single network cycle T_N is enough for each test. This approach has the benefits of comparing the SH and MH energy consumptions for the same network topology, enabling a separate study of the packet losses due to the synchronization drifts from those due to the P_{RF} dropping below the sensitivity threshold, and the repeatability of the results.

3.1 Network Topologies and Body Links Characterization

A preliminary characterization of the network topology in terms of link cost and time variability is performed. Per each link (e.g. γ_{13}), a data packet was sent every 1 second at 0 dBm of transmit power, for an observation time of 2 minutes. Each measurement was repeated 3 times and data were merged in a single history vector for each link. Per each packet, a RSSI measurement based on the Zigbee standard was stored and the path losses statistics are derived these values. While taking measurements, the volunteer was allowed to perform changes in the posture, as naturally happens in such scenario. Figure 3 shows the averaged RSSI and received power from measurements of the sitting postural set-up. Higher RSSI values correspond to a lower link costs. In case of SH scheme, the sensors 1, 2, 3, and 4 can only transmit directly to the sink.

In case of MH scheme, the routing protocol sets the sensor 1, 2 and 4 to communicate directly to the sink, as these links have a lower link cost if compared with any other MH link combination. The sensor 3 transmits to the sensor 4 and the latter acts as relay. In fact, considering the RSSI, the γ_{S3} link cost (where S stands for sink) is higher than the sum of γ_{13} and γ_{4S} link costs (e.g. $(-16)+(-9)<(-30)$). This can potentially results in transmit a power margin for the sensor 3 of 14 dB if compared to the SH case. The P_{RF} values are not numerically suitable as link costs for the routing algorithm. In fact, the sum of any MH links combination will not be lower than the SH links, even for MH power-wise convenient routes. As discussed before, only the 4 links relative to the sink are of interest for both SH and MH, while γ_{34} is of interest for MH only. The L_S time histories of these links are shown in Fig. 4, while Table 1 shows the statistical parameters. The standard variation σ spans from 5 dB to 8.1 dB, while the power range is up to 66 dB.

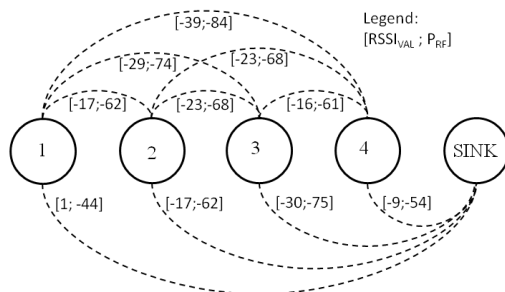


Fig. 3. Averaged RSSI and RF powers in dBm for sitting postural set-up

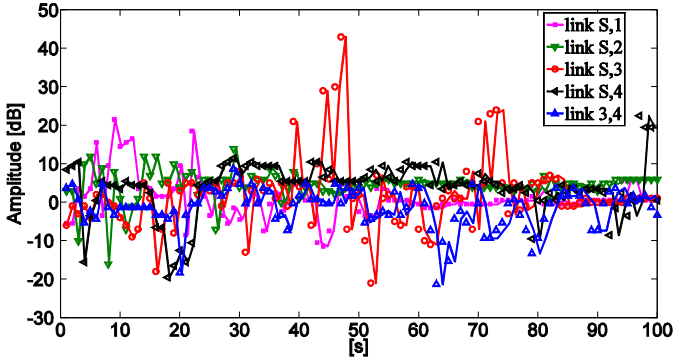


Fig. 4. Sample L_S history during the first 100 measurement seconds with sampling rate of 1 second

3.2 Network Packet Delivery Ratio (PRR) and Data Flow Rate Performances

From Table 1, the sensor 3 has M_0 of 20 and 34 dB for the SH and MH case, respectively. Moreover, σ is 8.1 and 5.0 dB for the γ_{S3} and γ_{34} cases, respectively. The probability of exceeding M_0 (or link blockage probability) is about $7 \cdot 10^{-3}$ for the SH and about $5 \cdot 10^{-12}$ for the MH case. Thus, a γ_{S3} blockage is significantly more likely than a γ_{34} link blockage. Figure 5 shows the SH PRR (primary y-axis on the right) and r (secondary y-axis on the left) for γ_{S3} with and without link blockage. The results are compared with the MH PRR and r with no link blockage on the γ_{34} link. The cases for $T_w = 93.75$ and 250 ms are considered. The PRR is > 0.9 for both SH and MH schemes with no links blockage. In case of MH network, it is shown the capability of sensor 4 to receive and route to the sink at least the data from the sensor 3 with a PRR comparable (e.g. $PRR > 0.9$) to the SH case with no blockage. In case of γ_{S3} link blockage, the SH PRR degrades of about 23% compared to the MH with no link blockage for both T_w cases, while the SH r reduction is 21% and 25% for the T_w case of 93.75 ms and 250 ms, respectively. This means that the MH topology can be used to overcome SH link blockages theoretically without PRR degradation, as the MH lower r compared to SH scheme is merely due to the synchronization basic approach discussed beforehand and it will be deepened later in this section.

As mentioned in Section 2, the PRR (and consequently r) depends directly on the waiting time (T_w) value. For this reason, both the PRR and r are preliminary studied against the T_w to maximize the data r while keeping at minimum the packet losses. Figure 6 compares the measured PRR (primary y-axis on the right) and the r (secondary y-axis on the left) against T_w for a SH and MH schemes with the link costs as defined in Table 1. The average per each sensor and the total network r are included. For $T_w \geq 93.75$ ms, the PRR is ≥ 0.9 for both schemes.

Table 1. Average path loss, available margins and statistical parameters of L_S per each link of interest

Link	L_{AVG} [dB]	M_0 [dB]	L_S [dB]			
			σ	Range	Min.	Max.
γ_{S1}	-44	24	7.2	53	-31.4	21.52
γ_{S2}	-62	42	6.7	43	-25.11	17.89
γ_{S3}	-75	20	8.1	66	-23.02	42.98
γ_{S4}	-54	34	7.4	44	-21.57	22.43
γ_{S4}	-61	41	5.0	32	-21.33	10.67

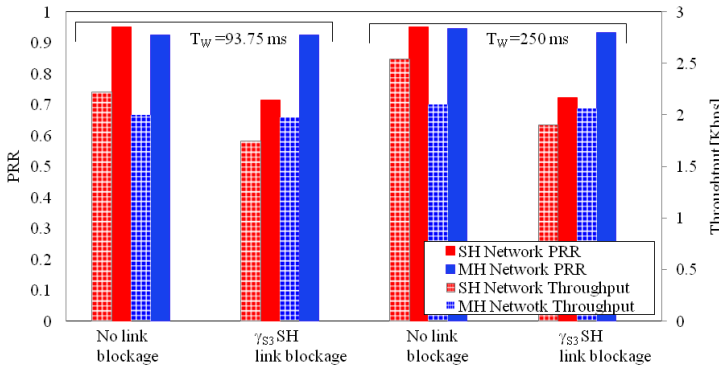


Fig. 5. Total Packet Delivery and throughput r for the SH and MH cases

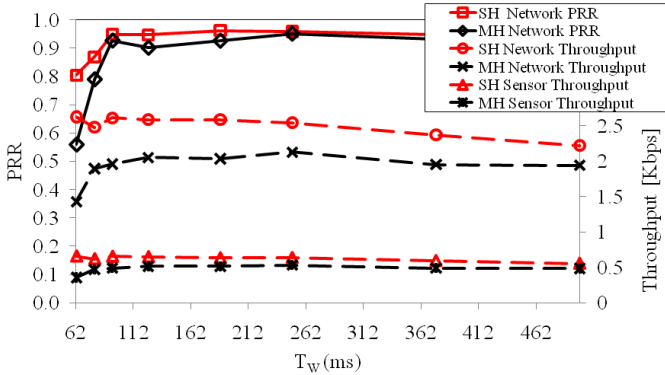


Fig. 6. PRR, total and average r against T_w for SH and MH schemes

3.3 Analytic Energy Consumption Analysis

As path loss L_S can change significantly in time even for sitting postural because of body movements, it is important to compare M against the energy consumption. The relationship between the transmit power and the sensor current consumption is not

linear. The energy consumption can be estimated as a function of data packets transmitted, based on the exact circuitry being used. As a 1.8V chipset voltage is used and the defined bit rate is 250 Kbps [22], \tilde{E}_{rx} is 135.4 nJ/bit, while \tilde{E}_{tx} at $P_T = 0$ dBm is 125.28 nJ/bit. The microcontroller energy costs are not considered. From [22], the current consumption in idle and sleep modes are significantly smaller ($>500\mu\text{A}$) compared to the maximum transmit and receive currents (17.7 and 18.8mA, respectively) and they are not considered neither.

The energy consumptions estimation only represents the energy per bit dissipated in the transceiver. As the extra energy dissipated during overhead processing (data generation, data serializations, etc.) and the media access control (MAC) related (such as the waiting time T_w) are not considered, this approach provides more general results as the energy is approximate using only the network topology, the transmitted power, the chipset implementation, the bitrates and the target reliability. The energy consumption at sensor 4 is estimated using formula (7) and with $n=1$. In MH case, the sensor 4 receives and retransmits the 75 bytes sent from sensor 3.

4 Conclusions

In this paper the potential benefits and limitations of cooperative networks as a means of augment the reliability in body-wearable sensor are studied. These trade-offs have been quantified for a sensor network prototyping a real-world platform for continuous ECG healthcare monitoring. For a packet delivery ratio >0.9 , the MH scheme can provide the network with a margin gain up to 14 dB traded off with an energy demand up to 30.7% higher and an average sensors r 20% lower than a SH scheme. The network lifetime of the MH scheme ranges from the 27% to 45% of the SH lifetime in cases of 0 dB and 20 dB margins, respectively. This work is a first exercise step in assessing reliability and life time trade-off with real-world platforms for body area sensor networks. Follow-up studies will address wireless ECG emulators with higher number of sensors (e.g. up to 10 for a typical 12-leads ECG system) employing ultra-low power chipsets in different specific health monitoring environments, such as critical care in hospitals, aged care or athlete monitoring.

References

1. IEEE std. 802.15.4 - 2003: Wireless Medium Access Control (MAC) and Physical Layer (PHY)
2. Otto, C., Milenkovic, A., Sanders, C., Jovanov, E.: System Architecture of a Wireless Body Area Sensor Network for Ubiquitous Health Monitoring. *Journal of Mobile Multimedia* 1(4), 307–326 (2006)
3. Jovanov, E., Milenkovic, A., Otto, C., De Groen, P.C.: A wireless body area network of intelligent motion sensors for computer assisted physical rehabilitation. *Journal of NeuroEngineering and Rehabilitation* 2, 6 (2005)
4. Yazdandoost, K.Y., et al.: Channel models for body area network, IEEE P802.15-08-0780-08-0006 (April 2009)

5. Strömmer, E., Hillukkala, M., Ylisaukkoja, A.: Ultra-low Power Sensors with Near Field Communication for Mobile Applications. Presented at 2007, Int. Conf. on Wireless Network, Las Vegas, Nevada (2007)
6. Sagan, D.: RF Integrated Circuits for Medical Applications: Meeting the Challenge of Ultra Low Power Communication. In: Ultra-Low-Power Communications Division, Zarlink Semiconductor, San Diego, CA (2005)
7. Falck, T., Baldus, H., Espina, J., Klabunde, K.: Plug 'n play simplicity for wireless medical body sensors. *Mobile Networks and Applications* 12(2-3), 143–153 (2007)
8. Mikami, S., Matsuno, T., Miyama, M., Yoshimoto, M., Ono, H.: A Wireless-Interface SoC Powered by Energy Harvesting for short range data communication, for Short range Data Communication. In: Proceedings of the 2005 IEEE Asian Solid-State Circuits Conference, Hsinchu, Taiwan, pp. 241–244 (2005)
9. Moerman, I., Blondia, C., Reusens, E., Joseph, W., Martens, L., Demeester, P.: The Need for Cooperation and Relaying in Short-Range High Path Loss Sensor Networks. In: Proc. of the 2007 IEEE Int. Conf. on Sensor Technologies and Applications, Washington, DC, pp. 566–571 (2007)
10. Chen, Y., Teo, J., Lai, J.C.Y., Gunawan, E., Low, K.S., Soh, C.B., Rapajic, P.B.: Cooperative communications in ultra-wideband wireless body area networks: channel modelling and system diversity analysis. *IEEE J. Sel. Areas Commun.* 27(1), 5–16 (2009)
11. Latre, B., Braem, B., Moerman, I., Blondia, C., Reusens, E., Joseph, W., Demeester, P.: A low-delay protocol for multihop wireless body area networks. In: Proc. of 4th Int. Conf., MobiQuitous, pp. 1–8 (2007)
12. Braem, B., Latré, B., Benoît, M., Blondia, C., Demeester, P.: The wireless autonomous spanning tree protocol for multi-hop wireless body area networks. Presented at 2006, 3rd Annual International Conference on Mobile and Ubiquitous Systems, San Jose, CA (2006)
13. Su-Ho, S., Gopalan, S.A., Seung-Man, C., Ki-Jung, S., Jae-Wook, N., Jong-Tae Park, P.: An energy-efficient configuration management for multi-hop wireless body area networks. In: 3rd IEEE Int. Conf. on Broadband Network and Multimedia Technology, pp. 1235–1239 (2010)
14. Djenouri, D., Balasingham, I.: New QoS and Geographical Routing in Wireless Biomedical Sensor Networks. In: Proc. of the 6th Int. Conf. on Broadband Communications, Networks, and Systems, Madrid, Spain, pp. 1–8 (2009)
15. Felemban, E., Lee, C.-G., Ekici, E.: MMSPEED: Multipath multi-speed protocol for QoS guarantee of reliability and timeliness in wireless sensor networks. *IEEE Transaction on Mobile Computing* 5(6), 738–754 (2006)
16. Razzaque, A., Alam, M.M., Or-Rashid, M., Hong, C.S.: Multi-constrained QoS geographic routing for heterogeneous traffic in sensor networks. *IEICE Trans. on Communications* 91B(8), 2589–2601 (2008)
17. Chipara, O., He, Z., Xing, G., Chen, Q., Wang, X., Lu, C., Stankovic, J., Abdelzaher, T.: Real-time power aware routing in sensor networks. In: Proc. of the IEEE 14th International Workshop on Quality of Service, pp. 83–92 (2006)
18. Sapiro, A., Tsouri, G.R.: Low-Power Body Sensor Network for Wireless ECG Based on Relaying of Creeping Waves at 2.4GHz. In: International Workshop on Wearable and Implantable Body Sensor Networks, pp. 167–173 (2010)
19. Heinzelman, W.R., Chandrakasan, A., Balakrishnan, H.: Energy-efficient communication protocol for wireless microsensor networks. In: Proc. of the 33rd Annual Hawaii Int. Conf. on System Sciences, January 4-7, vol. 2, p. 10 (2000)

20. Xigang, H., Hangguan, S., Xuemin, S.: On energy efficiency of cooperative communications in wireless body area network. Presented at 2011 IEEE Wireless Communications and Networking Conference, pp.1097–1101 (March 2011)
21. ZigBee RF transceiver datasheet, <http://www.ti.com/lit/ds/symlink/cc2420.pdf>
22. Sentilla webpage, <http://www.sentilla.com/blogs/2008/05/sentilla-announces-worlds-smal.php>
23. Fan, Y., Songwu, L., Lixia, Z.: A Scalable Solution to Minimum Cost Forwarding in Large Sensor Networks. In: Proc. of 10th Int. Conf. Comp. Communications and Networks, pp. 304–309 (2001)
24. Holland, M.M., Aures, R.G., Heinzelman, W.B.: Experimental investigation of radio performance in wireless sensor networks, Presented at 2nd IEEE Workshop on Wireless Mesh Networks, pp.140–150 (2006)
25. Madan, R., Lall, S.: Distributed algorithms for maximum lifetime routing in wireless sensor networks. IEEE Transactions on Wireless Communications 5(8), 2185–2193 (2006)
26. Bradie, B.: Wavelet packet-based compression of single lead ECG. IEEE Trans. Biomed. Eng. 43(5), 493–501 (1996)
27. Sha, K., Shi, W.: Modeling the lifetime of wireless sensor networks. Sensor Letters 3, 1–10 (2005)
28. Barsocchi, P., Oligeri, G., Potortì, F.: Measurement-based frame error model for simulating outdoor Wi-Fi networks. IEEE Transactions on Wireless Communications 8(3), 1154–1158 (2009)